Hindawi Publishing Corporation
Journal of Nanotechnology
Volume 2014, Article ID 212694, 8 pages
http://dx.doi.org/10.1155/2014/212694

Research Article

Enhanced Photocatalytic Performance of NiO-Decorated ZnO Nanowhiskers for Methylene Blue Degradation

I. Abdul Rahman, M. T. M. Ayob, and S. Radiman

School of Applied Physics, Faculty of Science & Technology, Universiti Kebangsaan Malaysia, 43600 Bangi, Selangor, Malaysia

Correspondence should be addressed to I. Abdul Rahman; irman@ukm.edu.my

Received 23 July 2014; Revised 7 November 2014; Accepted 11 November 2014; Published 25 November 2014

Academic Editor: Yoke K. Yap

Copyright © 2014 I. Abdul Rahman et al. This is an open access article distributed under the Creative Commons Attribution License, which permits unrestricted use, distribution, and reproduction in any medium, provided the original work is properly cited.

ZnO nanowhiskers were used for photodecomposition of methylene blue in aqueous solution under UV irradiation. The rate of methylene blue degradation increased linearly with time of UV irradiation. 54% of degradation rate was observed when the ZnO nanowhiskers were used as photocatalysts for methylene blue degradation for 80 min under UV irradiation. The decoration of p-type NiO nanoparticles on n-type ZnO nanowhiskers significantly enhanced photocatalytic activity and reached 72% degradation rate of methylene blue by using the same method. NiO-decorated ZnO was recycled for second test and shows 66% degradation from maximal peak of methylene blue within the same period. The increment of photocatalytic activity of NiO-decorated ZnO nanowhiskers was explained by the extension of the electron depletion layer due to the formation of nanoscale p-n junctions between p-type NiO and n-type ZnO. Hence, these products provide new alternative proficient photocatalysts for wastewater treatment.

1. Introduction

Nowadays, quality of water has become a major concern worldwide due to increasing population. Due to this reason, the proficient treatment of wastewaters has attracted major attentions among researchers around the globe to solve those problems. Ideally, the wastewater treatment process should be cost-effective and feasible for large-scale applications. The overall benefits of the wastewater treatment could save a huge amount of water and the treated water may be recycled or reused in applications such as textile industries, factory, or agriculture. Recently, the utilization of oxide semiconductor nanomaterials as effective photocatalysts in wastewater treatment has become a subject of major concern. Among oxide semiconductors, zinc oxide was chosen as a semiconducting photocatalyst for pollution abatement in water because it has strong oxidizing power, abundance, low cost, photostability, and large exciton binding energy of 60 MeV [1]. It also has a direct band gap energy at 3.37 eV at room temperature, making it a suitable candidate in absorbing UV-light as an excitation source [2]. ZnO-based photocatalysts have attracted much attention because of their chemical stabilizations, its nontoxicity, being cost-effective, and being environment-friendly [3]. Several researchers reported that zinc oxide has good photocatalytic activity and shows the appropriate activity in the range of solar radiation [4–6].

The efficiency of photocatalytic activity by ZnO would be further improved by controlling donor density, selecting the synthesis methods, and varying electronic interaction between new compound like the composite and doped ZnO [7–9]. In particular, when p-type oxide materials such as NiO are added to n-type oxide material such as ZnO, the p-type NiO can either incorporate into n-type ZnO or form second phase. Thus, the incorporation of NiO into the lattice of ZnO and the formation of a secondary form with ZnO will have a completely different impact on the photodegradation behavior like a changing in donor density and an extension of the electron depletion layer near the interface of the p-n type junction, correspondingly.

Among all synthesis methods, the sonochemistry process is particularly attractive due to the following reasons: low equipment cost and fast and large-scale production [10]. Surfactants can also play an important role as capping agent in synthesizing the material to control the size, shape, and

agglomeration among the particles to give different interesting morphologies [11]. In this study, we have controlled the sonication process and the growth of nuclei by employing good absorption of the triethanolamine (TEA) onto the surface of the particles. TEA is an interesting ligand which is both a tertiary amine and a triol with a lone pair of electrons on the nitrogen atom [12]. The aim of this study is to examine the effect, stability, and recyclability of new NiO-ZnO nanocomposites (NCs) via decoration of n-type ZnO nanowhiskers (NW) networks with discrete form of p-type NiO nanoparticles (NP) to meet the demands of ZnO NWs as a photocatalyst on the photocatalytic activity by using UV irradiation in the methylene blue (MB) solution. The degradation of methylene blue was monitored by UV-Vis spectrometer, and the reaction rates were calculated from the measured absorbance.

2. Experimental Detail

2.1. Materials. Zinc nitrate hexahydrate, reagent grade, 98%, purchased from Merck, nickel(II) nitrate hexahydrate, reagent grade ≥98.5%, purchased from Sigma Aldrich, sodium hydroxide, ACS reagent, ≥97.0%, pellets, also purchased from Sigma Aldrich, and methylene blue trihydrate, ≥99%, purchased from Mallinckrodt, were used for the evaluation of the photocatalytic activity. All chemicals were analytical grade reagents and used without further purification.

2.2. Synthesis of NiO Nanoparticles, ZnO Nanowhiskers, and NiO-ZnO Nanocomposites. To obtain the NiO NPs and ZnO NWs, 1.3072 g of $Zn(NO_3)_2{\cdot}4H_2O$ (0.1 mol), 0.5816 g of $Ni(NO_3)_2{\cdot}6H_2O$ (0.1 mol), and 0.56 g of NaOH (0.2 mol) were dissolved in deionized water for each sample and magnetically stirred at room temperature for 10 min. The triethanolamine (TEA) was poured into each solution with molar ratio 1 : 3 of excess TEA and continued stirring for 20 min. To produce NiO-ZnO NCs, the 10% of $Ni(OH)_2$ solution was mixed into $Zn(OH)_2$ solution with continued stirring for 20 min. NaOH solution was added dropwise to each solution during the high-intensity ultrasound irradiation process (misonix-400, 60 Hz, 70 amplitude) for 60 min. The parameter of frequency and time sonication were controlled to get a proper shape of each nanoparticle. The sample was centrifuged, washed with excess deionised water, and dried at 60°C for 12 hours in the oven. The crystallinity and morphology of the products were characterized by XRD (Bruker X-ray diffractometer, scanning rate 0.01°/s, Cu-Kα radiation, and λ = 0.154 nm) and TEM (Hitachi H-7100 with operating voltage 100 kV) instruments. The band gap energies of the products were analyzed using UV-Vis spectroscopy (Perkin-Elmer Lambda 35 equipped with xenon flash lamp for best sensitivity) and also used for monitoring the absorption of methylene blue. Excitation and emission measurements were performed at room temperature and photoluminescence intensity was measured by FLS-920 spectrophotometer (excitation wavelength: 325 nm). The bonding form of each structure was investigated using Fourier transform infrared spectroscopy (Perkin Elmer/Lamda 950).

2.3. Photocatalytic Activity Preparation. The photocatalytic activities of the samples were determined by measuring the degradation of MB solution under simulated UV irradiation. At first, 50 mg of photocatalysts was immersed into a beaker filled with 50 mL MB solution (10 mg/L). Then this solution was stirred continuously at 25°C and meanwhile irradiated by using UV-lamp (UVP-UVLMS-38, United States) which is operating at a power of 8.0 W and placed 10 cm above the conical flask to provide irradiance wavelength of 365 nm with intensity of 950 $\mu W/cm^2$. Each 5 mL of the solution was centrifuged at 4000 rpm for 10 min to separate the photocatalysts from the suspense every 20 min during UV irradiation in order to determine the degree of degradation of MB by using UV-visible spectrophotometer.

3. Results and Discussion

3.1. Morphology. The morphology, structure, and size of the samples obtained using sonochemistry method were examined using TEM. Figure 1(a) shows a whiskers-like shape with a clean surface for ZnO NWs with a size of approximately 50 × 1300 nm (width × length) which were identified as single crystalline. In the chemical reaction, $Zn(NO_3)_2{\cdot}4H_2O$ was reacted with NaOH in the presence of triethanolamine. During the experiment, there were many white floccules produced during mixing process. We believe that the TEA has a great influence on ZnO nanowhiskers. According to Flory-Huggins theory, TEA solutes with the limited water can form chains structure [13]. The surfactant molecules assemble into micelle if the concentrations of surfactant molecules are high enough. Thus, these TEA solutes wrap around the ZnO nanoparticles when grown up along these chains. ZnO nanowhiskers may be obtained after reaction processes were completed. Ellipsoids-like morphology with discrete form was observed for NiO NPs as shown in Figure 1(b) with an average diameter of approximately 40 nm. An image of the NiO-decorated ZnO NWs sample in Figure 1(c) shows a composite structure consisting of irregular NiO nanostructures which attach to ZnO NWs surface and constitute the rods-like structures. The dark regions in that figure are ZnO particles because ZnO has a higher electron density and therefore a higher contrast than NiO particles. The size and morphology of ZnO particles increased and changed after decoration from NiO NPs, which is caused by crystal growth and sintering occurring during preparation process. It can be seen that the average grain size of the NiO-ZnO sample was about 0.1 × 1.3 μm (width × length). The introduction of NiO into ZnO solution leads to large structural strain, which causes the origination of stacking faults on the ZnO NWs and strongly affects their optical, electrical, and possibly chemical properties [14]. It is concluded that the rod shape of NiO-ZnO NCs is composed of whiskers-like ZnO nanostructures decorated by NiO NPs. Moreover, the space charge region is well constructed along the longitudinal direction of NiO-ZnO sample, meaning that photogenerated electrons can flow in the direction of the crystal length, resulting in higher activity compared with NiO and ZnO samples.

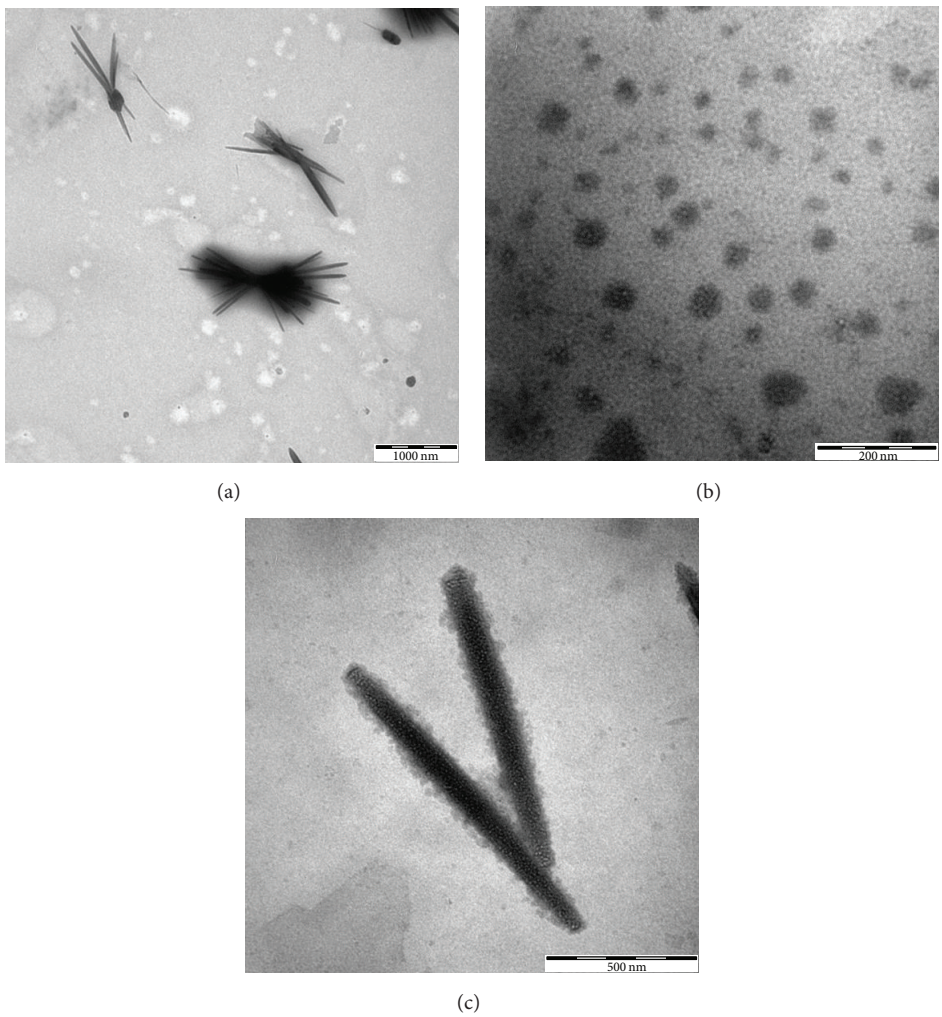

(a) (b)

(c)

Figure 1: TEM micrograph of (a) ZnO nanowhiskers, (b) NiO nanoparticles, and (c) NiO-ZnO nanocomposites.

3.2. Crystallinity. The phase formation was revealed by the XRD technique. Figure 2 shows the XRD patterns of the samples obtained before and after photocatalytic test on the photodecomposition of MB. There are not any significant changes after photocatalytic test. All the peaks in the XRD pattern of the ZnO NWs sample have been indexed to hexagonal wurtzite structure of ZnO (JCPDS Card number 036-1415) with the lattice parameters: $a = 0.3250$ nm, $c = 0.5207$ nm, and space group P63mc. NiO NPs were indicating a rhombohedral bunsenite structure of NiO (JCPDS Card number 044-1159) with the lattice parameters: $a = 0.4177$ nm and space group fm-3 m. The strong, sharp, and broadening diffraction peaks indicated that the products are well crystalline in nanometer scale. It was observed that the patterns of NiO-ZnO NCs were similar to the pattern of NiO NPs and ZnO NWs because the NiO NPs were formed on the ZnO NWs surface. This interesting finding demonstrates that the NiO-ZnO NCs are highly stable and exhibit excellent recyclability, suitable for photocatalytic applications.

3.3. Chemical Bonding. Fresh solutions of each sample were examined via FTIR analysis. From Figure 3, the spectrum for NiO, ZnO, and NiO/ZnO shows a common broad peak in the range of 2800 to 3500 cm^{-1}, attributed to the O–H stretching bond. An asymmetric and symmetric C–H stretching bond for NiO, ZnO, and NiO/ZnO are observed at around 2975 cm^{-1}. C–H vibrations (wagging, twisting) for each sample were observed at 1382 cm^{-1} to 1415 cm^{-1} [15]. A small peak at around 1089 cm^{-1} indicates the C–N stretching bonds for all samples [16]. A sharp band at around 881 cm^{-1} is caused by C–O bond stretching [15]. The intense band at 444 cm^{-1} may be assigned to the Ni–O stretching. Meanwhile, Zn–O bond vibrates at 436 cm^{-1} forming an intense band [16]. It is proposed that, in the mechanism of metal oxides synthesis from metal nitrates and TEA, the product of NiO and ZnO is obtained considering the FTIR spectra.

3.4. Absorption. In order to investigate the optical properties of NiO NPs, ZnO NWs, and NiO-ZnO NCs, UV-Vis measurements were conducted at room temperature. Figure 4(a) shows the UV-Vis absorption spectrum of the samples synthesized by using ultrasonic radiation. Broad absorption peaks can be found in the range of 300–500 nm. There are two

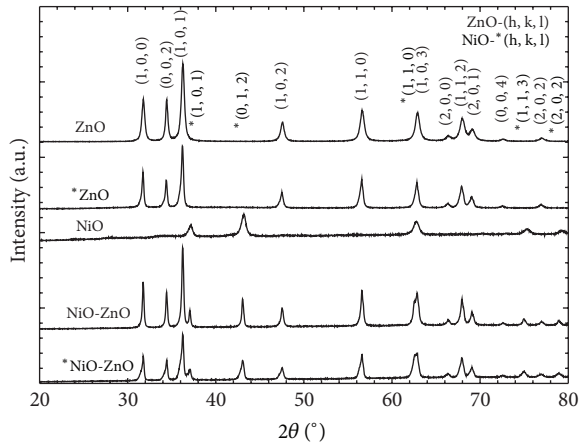

Figure 2: XRD pattern of the ZnO nanowhiskers, NiO nanoparticles, and NiO-decorated ZnO nanocomposites before and (∗) after photocatalytic test on the photodecomposition of MB.

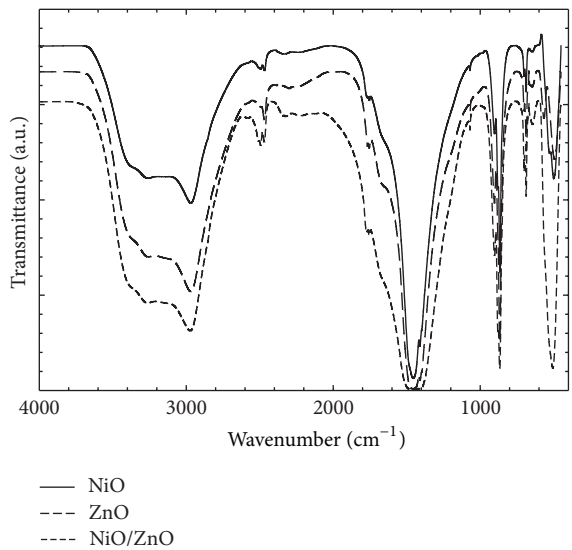

Figure 3: FTIR spectra of NiO nanoparticles, ZnO nanowhiskers, and NiO-ZnO nanocomposites.

prominent absorption peaks for NiO-ZnO NCs, which can be assigned to the characteristic absorption of ZnO NWs and NiO NPs component, respectively. This also confirms that the NiO-ZnO sample is a composite material composed of NiO and ZnO. The absorption intensity of ZnO is much higher than that of NiO, confirming that the composite is composed of more ZnO than NiO in amount. The absorption wavelength of each sample was blue-shifted compared to their bulk structure, considering the quantum confinement effect due to size reduction of nanoparticles [1]. The blue shift denotes the decrease in size of particle and increase in band gap energy. The band gap energy, E_g, values for NiO NPs, ZnO NWs, and NiO-ZnO NCs are 2.82, 3.56, and 3.69 eV, respectively, obtained by extrapolating the linear portion of the curve to $h\nu$ as shown in Figure 4(b).

In order to understand the photocatalytic mechanism of photocatalysts, it is essential to determine their energy-band potentials since the redox ability of photogenerated carriers is associated with energy-band potentials of photocatalysts. Martha et al. 2014 reported that the conduction band and valence band potential were calculated to be $E_{CB} = -0.17$ eV and $E_{VB} = +3.05$ eV [17]. When ZnO is irradiated with light of energy greater than its band gap energy, electrons from valence band were excited to the conduction band, creating e^-/h^+ pairs [18]. Generally, most of the photogenerated e^- and h^+ recombine rapidly, and only a few of them participate in redox reactions. It is noted that NiO, which is a p-type semiconductor and has a valence band maximum of ~0.4 eV below the Fermi level ($E_f = 5.0$ eV), is positive to the conduction band potential of ZnO (−0.17 eV) [19]. When ZnO particles are assembled onto NiO particles, the photogenerated electrons can readily transfer from the conduction band of ZnO to NiO via p-n junction. Thus, the recombination of electron-hole pairs can be effectively suppressed in the composites, which leads to an increased availability of electrons and holes for the photocatalytic reactions. The photogenerated e^- which transferred onto the NiO would react with O_2 and H^+ to produce H_2O_2, which are active for methylene blue dye degradation and also participate in the reactions to form $^*OH$. The valence band potential of ZnO (+3.05 eV) is positive to the redox potential of $OH^-/^*OH$ (+1.89 eV), indicating that the photogenerated h^+ can react with OH^- to produce $^*OH$ [20]. As a consequence, the active species of $^*OH$, h^+, and H_2O_2 work together to degrade methylene blue dye.

3.5. Photoluminescence. Figure 5 shows the comparison between photoluminescence spectra of the ZnO NPs and NiO/ZnO NCs excited at 325 nm. The main feature is composed of an excitation band at 325 nm and a corresponding emission at 442 nm (UV) and emission from 500 up to 700 nm with a band located around 550 nm and a second band around 660 nm. The luminescence at visible range has been attributed to defects such as oxygen vacancies, zinc vacancies, and donor/acceptor pairs [21]. The PL signal centered at around 442 nm is obviously detected for each sample, revealing the generation of $^*OH$ radicals. In the case of ZnO NWs, this may be due to the presence of surface defects which include nitrate and –OH groups [22]. When the NiO-ZnO NCs are used as the photocatalyst, the PL signal becomes more intense, suggesting that the yield of the $^*OH$ radicals is enhanced over the irradiated composites. Generally, h^+, $^*OH$, and H_2O_2 are thought to be the main active species responsible for the dye degradation [23].

3.6. Photocatalytic Activity. Photocatalytic degradation of MB in an aqueous suspension of the ZnO NWs and NiO-ZnO NCs was performed to evaluate their photocatalytic activity. The photodecomposition of the MB was investigated under the simulated UV irradiation. Figure 6 demonstrates the photocatalytic degradation activity of MB concentrations as the effects of photodecomposition initiated by ZnO NWs (Figure 6(a)) and NiO-decorated ZnO NCs (Figures 6(b) and

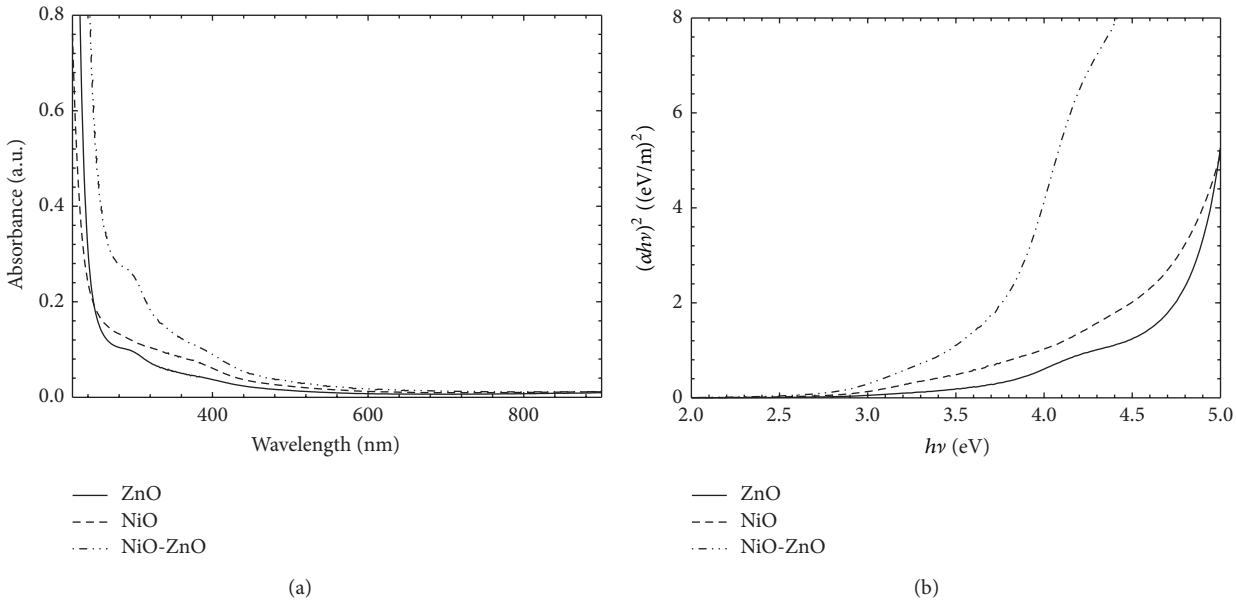

Figure 4: UV-Vis spectrum of (a) fresh solution absorption and (b) curve of $(\alpha h\nu)^2$ against $h\nu$ for NiO NPs, ZnO NWs, and NiO-ZnO NCs.

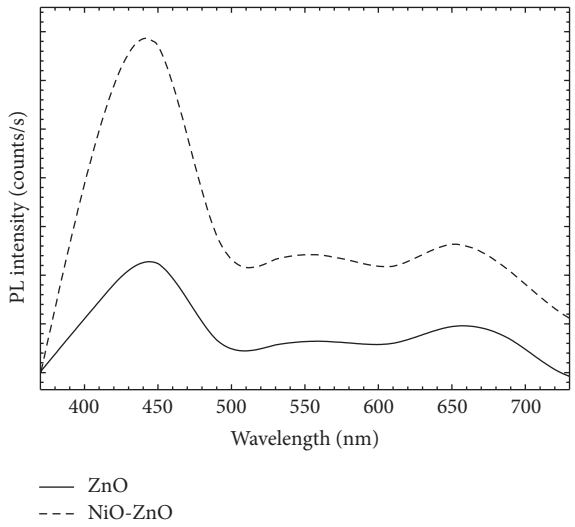

Figure 5: Photoluminescence spectra of the ZnO and NiO-ZnO samples.

6(c)) after being irradiated in UV-lamp for 80 min. The intensity absorption peak of MB at 665 nm decreased gradually with the extension of time, indicating the degradation of chromosphere group of MB [24]. Moreover, the diminished intensities of blue colour in MB solution imply that all or part of the auxochromic groups (methyl or methylamine) has degraded through demethylation and hydroxylation process [25, 26]. The detailed mechanism of the photocatalytic process on the ZnO NWs and NiO-decorated ZnO NCs is tha t both photocatalytic oxidative and reductive reactions occur simultaneously on both particles. When the ZnO NWs are irradiated by UV-radiation, the electron-hole pairs were produced generated by excitation of the electron from valence band to conduction band in ZnO NWs. The holes created in the valence band can react with water molecules to give hydroxide radicals (*OH). The redox potential of the electron-hole pair permits H_2O_2 formation. Several issues are important to understand in this process. First, the oxidizing species cannot migrate for a long distance and stay near the active sites. Second, the recombination of positive holes with excited electron before they react to create active species and centers has to be avoided. Additionally, the ZnO NWs loaded with NiO NPs in the NiO-ZnO NCs should not decrease or change under repeated cycles and must be easy to separate from MB in aqueous solution. The NiO-decorated ZnO NCs could be recycled many times, but only the first five cycles showed impressive results. Figures 5 and 6 show the pseudo-first order assumption describes the photodegradation data well.

Figure 7 shows the efficiency comparison for ZnO NWs, NiO-ZnO NCs, and NiO-ZnO NCs recycled as a function of irradiation times. To demonstrate the favorable photocatalytic activity induced by the synergistic effect of the coupled NiO-ZnO NCs, the photodegradation of MB was compared with ZnO NWs. There is only slight decrease to 54% for ZnO NWs compared to 72% for NiO-ZnO NCs from maxima absorption after UV irradiation for 80 min. The NiO-ZnO NCs recycled also exceed ZnO with 66% degraded of MB for the same period, which means attendance of NiO would increase the efficiency of photodecomposition process due to the coexistence of Ni^{3+} and Ni^{2+} ionic compounds [27]. The tiny loss of the photocatalytic efficiency indicates the excellent photocatalytic reusability of the as-prepared NiO-ZnO NCs. Additionally, the decoration of p-type NiO NPs on ZnO NWs increased photocatalytic activities by extension of electron depletion layer near the p-n junction and greatly enhanced the responses to MB. Thus, for NiO-ZnO NCs, the photoresponse ranges are extended, and more light energy could be

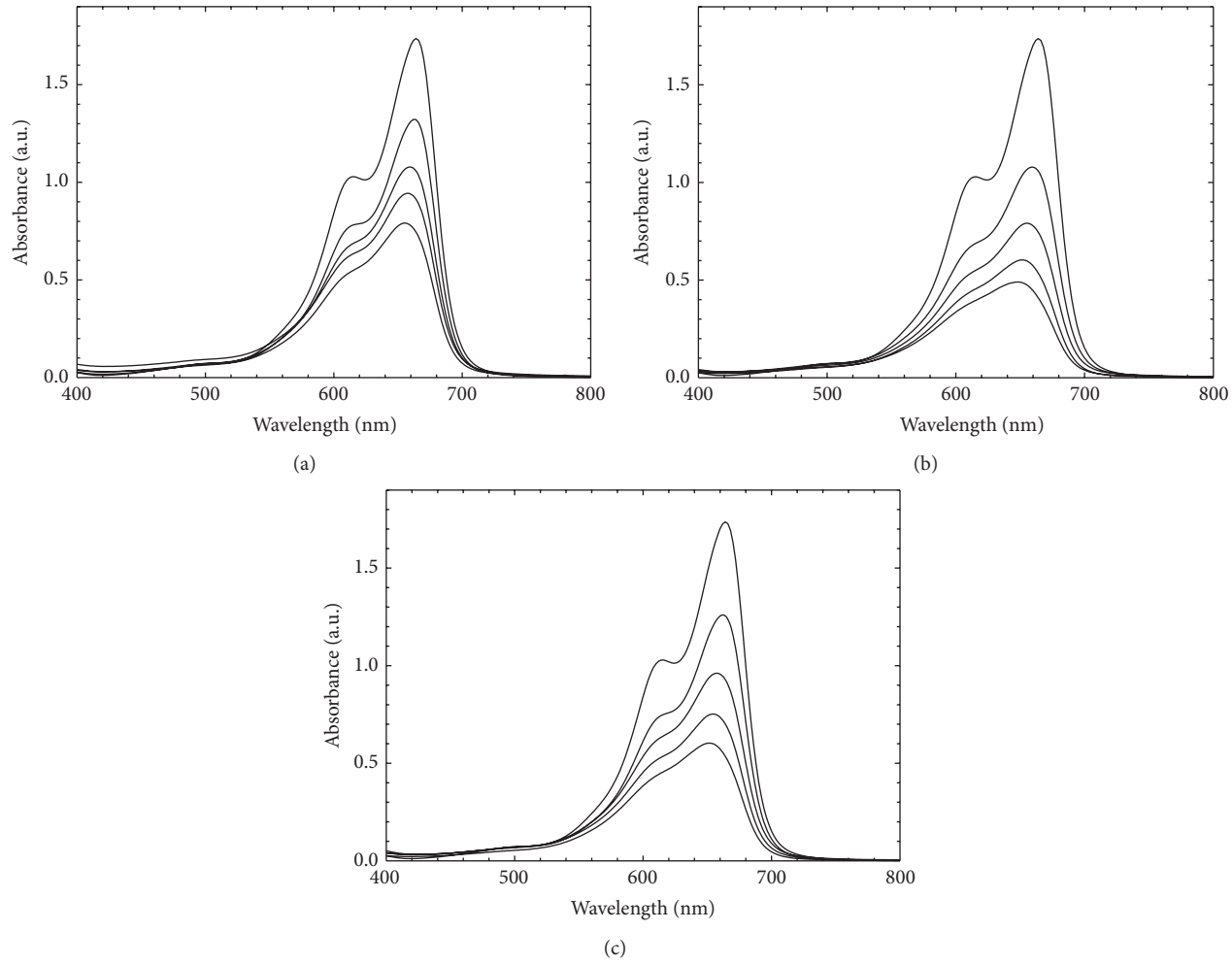

Figure 6: The photocatalytic degradation activity of MB concentrations for (a) ZnO NWs, (b) NiO-decorated ZnO NCs, and (c) NiO-decorated ZnO NCs recycled.

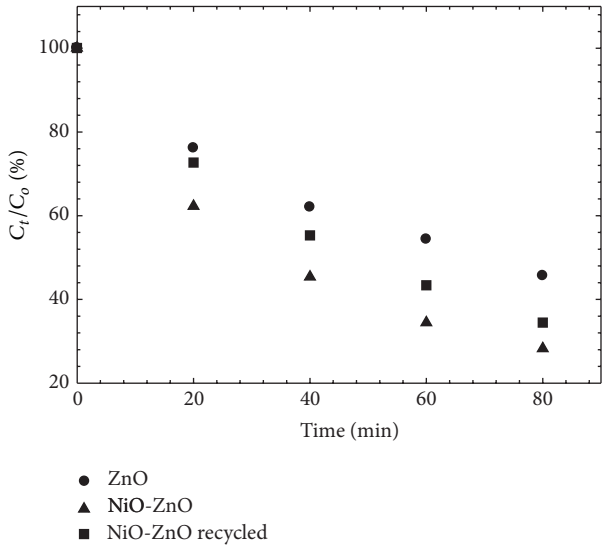

Figure 7: Relative amounts of methylene blue degraded versus time for ZnO NWs, NiO-ZnO NCs, and NiO-ZnO NCs recycled.

utilized compared to ZnO NWs under the simulated UV light irradiation. The photocatalytic activities of the samples can also be quantitatively evaluated by comparing the first order reaction rate constant (k) as shown in Figure 6.

In order to elucidate the reaction rates, the data were replotted in $\ln(C_o/C_t)$ versus time as shown in Figure 8. All the photocatalytic reactions are almost approaching pseudo-first order reaction with precisely R-squared values of 0.982, 0.974, and 0.995 for ZnO NWs, NiO-ZnO NCs, and NiO-ZnO NCs recycled, respectively. In accordance with the MB with ZnO NWs, the rate constant gave the k-value of 0.009 min^{-1} (Figure 6(c)) while this value increased to 0.015 min^{-1} (Figure 8(a)) after using NiO-ZnO NCs as photocatalysts and reduced to 0.013 min^{-1} (Figure 8(b)) after being recycled by calculating the slope of the graph. The decrement of the rate constant of NiO-ZnO NCs recycled could be attributed to the decreased efficiency rate of absorbance MB in solution that is caused by reduced correspondence to the electron transition compared to original NiO-ZnO NCs [28]. Another factor that affects the photocatalytic activity of

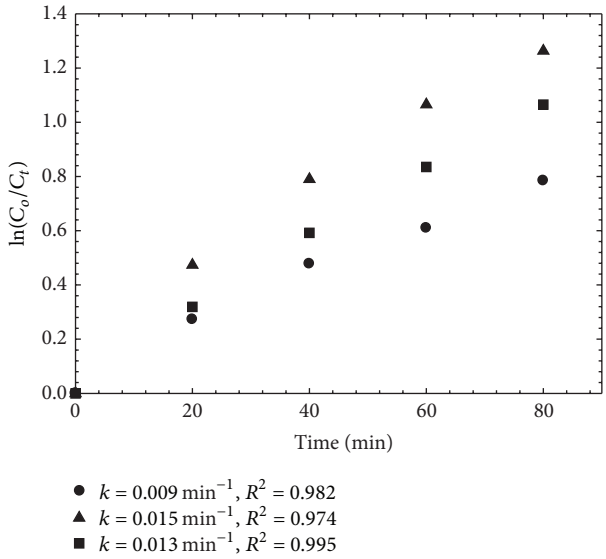

FIGURE 8: The concentration of methylene blue plotted as $\ln(C_o/C_t)$ versus time for (▲) NiO-ZnO NCs, (■) NiO-ZnO NCs recycled, and (●) ZnO NWs.

MB with NiO-ZnO NCs is polar planes and oxygen vacancies, which act as electron traps for photodegradation [29]. Mclaren et al. have demonstrated that a greater proportion of exposed polar surfaces lead to a greater photocatalytic activity [30]. They discovered that hydroxyl ions prefer to adsorb onto (0001)-Zn plane surface due to its surface positive charge, which can react with hole to generate *OH species, hence enhancing the photocatalytic activity.

4. Conclusion

ZnO, NiO, and NiO-ZnO nanopowders with whiskers-like, ellipsoids-like, and rod shape were successfully constructed by the sonochemical method. Adding $Ni(OH)_2$ to $Zn(OH)_2$ solution did alter the shape of ZnO from whiskers-like to rods-like shape with NiO particles deposited onto the surface of ZnO and the crystallite size becomes bigger than pure ZnO. From UV-Vis examined, the E_g values for NiO, ZnO, and NiO-ZnO are to be 2.82, 3.56, and 3.69 eV, respectively. The degradation efficiencies of ZnO under UV irradiation are greatly enhanced by forming NiO-ZnO nanocomposite. The efficiency photodegradation of MB with NiO-ZnO nanocomposites shows a significant 72% effectiveness of degradation compared to 54% from maxima absorption of ZnO for 80 min illumination. The NiO-ZnO was reused for second photocatalytic test and showed decrement of absorption MB to be 66% for the same parameter as before. The NiO-ZnO photocatalysts proposed in this work is a potential candidate to treat the wastewater from textile and other industries by using a simple method with the cheapest cost.

Conflict of Interests

The authors declare that there is no conflict of interests regarding the publication of this paper.

Acknowledgment

The authors wish to acknowledge funding for this study from Universiti Kebangsaan Malaysia, Grants DLP-2013-037 and UKM-DIP-2014-22.

References

[1] T. Alammar and A. V. Mudring, "Facile ultrasound-assisted synthesis of ZnO nanorods in an ionic liquid," *Materials Letters*, vol. 63, no. 9-10, pp. 732–735, 2009.

[2] Y. W. Chen, Q. Qiao, Y. C. Liu, and G. L. Yang, "Size-controlled synthesis and optical properties of small-sized ZnO nanorods," *Journal of Physical Chemistry C*, vol. 113, no. 18, pp. 7497–7502, 2009.

[3] L. Li, W. Wang, H. Liu, X. Liu, Q. Song, and S. Ren, "First principles calculations of electronic band structure and optical properties of Cr-doped ZnO," *Journal of Physical Chemistry C*, vol. 113, no. 19, pp. 8460–8464, 2009.

[4] C. Tian, Q. Zhang, A. Wu et al., "Cost-effective large-scale synthesis of ZnO photocatalyst with excellent performance for dye photodegradation," *Chemical Communications*, vol. 48, no. 23, pp. 2858–2860, 2012.

[5] R. Y. Hong, J. H. Li, L. L. Chen et al., "Synthesis, surface modification and photocatalytic property of ZnO nanoparticles," *Powder Technology*, vol. 189, no. 3, pp. 426–432, 2009.

[6] Y. Li, Z. Jiao, N. Yang, and H. Gao, "Regeneration of nano-ZnO photocatalyst by the means of soft-mechanochemical ion exchange method," *Journal of Environmental Sciences*, vol. 21, supplement 1, pp. S69–S72, 2009.

[7] J.-X. Sun, Y.-P. Yuan, L.-G. Qiu et al., "Fabrication of composite photocatalyst g-C_3N_4-ZnO and enhancement of photocatalytic activity under visible light," *Dalton Transactions*, vol. 41, no. 22, pp. 6756–6763, 2012.

[8] K. S. Yu, J. Y. Shi, Z. L. Zhang, Y. M. Liang, and W. Liu, "Synthesis, characterization, and photocatalysis of ZnO and Er-Doped ZnO," *Journal of Nanomaterials*, vol. 2013, Article ID 372951, 5 pages, 2013.

[9] P. Sathishkumar, R. Sweena, J. J. Wu, and S. Anandan, "Synthesis of CuO-ZnO nanophotocatalyst for visible light assisted degradation of a textile dye in aqueous solution," *Chemical Engineering Journal*, vol. 171, no. 1, pp. 136–140, 2011.

[10] Y. A. Kalandaragh, A. Khodayari, and M. Behboudnia, "Ultrasound-assisted synthesis of ZnO semiconductor nanostructures," *Materials Science in Semiconductor Processing*, vol. 12, no. 4-5, pp. 142–145, 2009.

[11] M. Pradhan, S. Sarkar, A. K. Sinha, M. Basu, and T. Pal, "High-yield synthesis of 1D Rh nanostructures from surfactant mediated reductive pathway and their shape transformation," *The Journal of Physical Chemistry C*, vol. 114, no. 39, pp. 16129–16142, 2010.

[12] Z. Boulsourani, G. D. Geromichalos, K. Repana et al., "Preparation and pharmacochemical evaluation of mixed ligand copper(II) complexes with triethanolamine and thiophenyl-2 saturated carboxylic acids," *Journal of Inorganic Biochemistry*, vol. 105, no. 6, pp. 839–849, 2011.

[13] J. M. G. Cowie, *Polymers: Chemistry and Physics of Modern Materials*, Chapman & Hall, London, UK, 2nd edition, 1991.

[14] Y. Ding and Z. L. Wang, "Structures of planar defects in ZnO nanobelts and nanowires," *Micron*, vol. 40, no. 3, pp. 335–342, 2009.

[15] C. S. Dandeneau, Y.-H. Jeon, C. T. Shelton, T. K. Plant, D. P. Cann, and B. J. Gibbons, "Thin film chemical sensors based on p-CuO/n-ZnO heterocontacts," *Thin Solid Films*, vol. 517, no. 15, pp. 4448–4454, 2009.

[16] M. Vafaee and M. S. Ghamsari, "Preparation and characterization of ZnO nanoparticles by a novel sol-gel route," *Materials Letters*, vol. 61, no. 14-15, pp. 3265–3268, 2007.

[17] S. Martha, K. H. Reddy, and K. M. Parida, "Fabrication of In_2O_3 modified zno for enhancing stability, optical behaviour, electronic properties and photocatalytic activity for hydrogen production under visible light," *Journal of Materials Chemistry A*, vol. 2, no. 10, pp. 3621–3631, 2014.

[18] X. Zhang, J. Qin, Y. Xue et al., "Effect of aspect ratio and surface defects on the photocatalytic activity of ZnO nanorods," *Scientific Reports*, vol. 4, article 4596, 2014.

[19] M. D. Irwin, D. B. Buchholz, A. W. Hains, R. P. H. Chang, and T. J. Marks, "*p*-Type semiconducting nickel oxide as an efficiency-enhancing anode interfacial layer in polymer bulk-heterojunction solar cells," *Proceedings of the National Academy of Sciences of the United States of America*, vol. 105, no. 8, pp. 2783–2787, 2008.

[20] T. Xian, H. Yang, L. Di, J. Ma, H. Zhang, and J. Dai, "Photocatalytic reduction synthesis of SrTiO3-graphene nanocomposites and their enhanced photocatalytic activity," *Nanoscale Research Letters*, vol. 9, pp. 327–336, 2014.

[21] A. van Dijken, E. A. Meulenkamp, D. Vanmaekelbergh, and A. Meijerink, "Luminescence of nanocrystalline ZnO particles: the mechanism of the ultraviolet and visible emission," *Journal of Luminescence*, vol. 87–89, pp. 454–456, 2000.

[22] H. K. Yadav, K. Sreenivas, V. Gupta, S. P. Singh, and R. S. Katiyar, "Effect of surface defects on the visible emission from ZnO nanoparticles," *Journal of Materials Research*, vol. 22, no. 9, pp. 2404–2409, 2007.

[23] W. Y. Teoh, J. A. Scott, and R. Amal, "Progress in heterogeneous photocatalysis: from classical radical chemistry to engineering nanomaterials and solar reactors," *The Journal of Physical Chemistry Letters*, vol. 3, no. 5, pp. 629–639, 2012.

[24] X. Shu, J. He, and D. Chen, "Tailoring of phase composition and photoresponsive properties of Ti-Containing nanocomposites from layered precursor," *Journal of Physical Chemistry C*, vol. 112, no. 11, pp. 4151–4158, 2008.

[25] T. Zhang, T. Oyama, A. Aoshima, H. Hidaka, J. Zhao, and N. Serpone, "Photooxidative *N*-demethylation of methylene blue in aqueous TiO_2 dispersions under UV irradiation," *Journal of Photochemistry and Photobiology A: Chemistry*, vol. 140, no. 2, pp. 163–172, 2001.

[26] T. Chen, Y. Zheng, J.-M. Lin, and G. Chen, "Study on the photocatalytic degradation of methyl orange in water using Ag/ ZnO as catalyst by liquid chromatography electrospray ionization ion-trap mass spectrometry," *Journal of the American Society for Mass Spectrometry*, vol. 19, no. 7, pp. 997–1003, 2008.

[27] H. He Jr., C. S. Lao, L. J. Chen, D. Davidovic, and Z. L. Wang, "Large-scale Ni-doped ZnO nanowire arrays and electrical and optical properties," *Journal of the American Chemical Society*, vol. 127, no. 47, pp. 16376–16377, 2005.

[28] X. Shao, W. Lu, R. Zhang, and F. Pan, "Enhanced photocatalytic activity of TiO_2-C hybrid aerogels for methylene blue degradation," *Scientific Reports*, vol. 3, article 3018, 2013.

[29] D. S. Bohle and C. J. Spina, "The relationship of oxygen binding and peroxide sites and the fluorescent properties of zinc oxide semiconductor nanocrystals," *Journal of the American Chemical Society*, vol. 129, no. 41, pp. 12380–12381, 2007.

[30] A. Mclaren, T. Valdes-Solis, G. Li, and S. C. Tsang, "Shape and size effects of ZnO nanocrystals on photocatalytic activity," *Journal of the American Chemical Society*, vol. 131, no. 35, pp. 12540–12541, 2009.

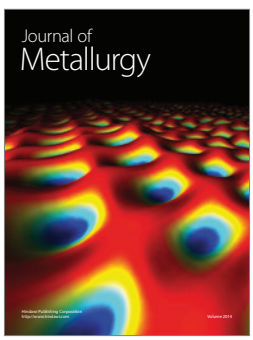

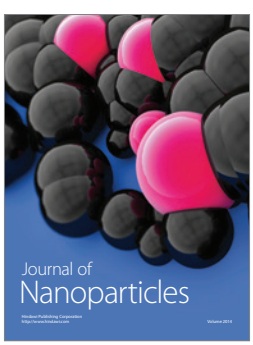

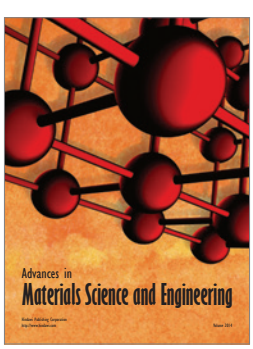

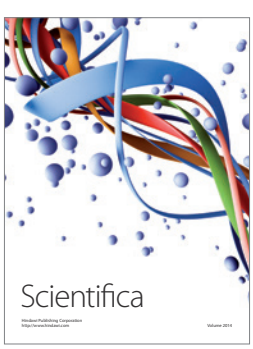

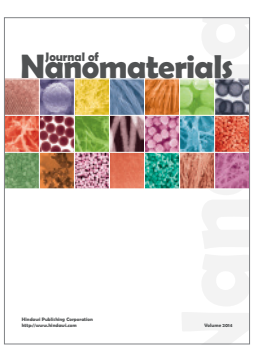

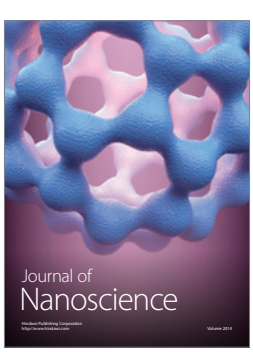

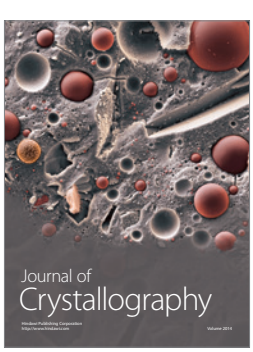

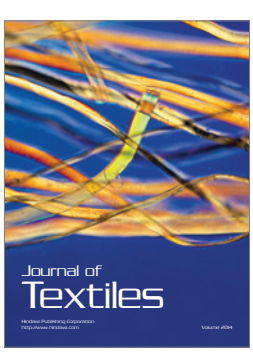

Hindawi

Submit your manuscripts at
http://www.hindawi.com